行政院國家科學委員會專題研究計畫　成果報告

鑭錳氧化物/(絕緣氧化物,導體)異質微粒複合物中晶界自旋極化穿隧效應與磁傳輸機制的探討

計畫類別：個別型計畫
計畫編號：NSC93-2112-M-164-003-
執行期間：93 年 08 月 01 日至 94 年 07 月 31 日
執行單位：修平技術學院電機工程系

計畫主持人：楊尚霖

計畫參與人員：謝承達，張國興

報告類型：精簡報告
報告附件：出席國際會議研究心得報告及發表論文
處理方式：本計畫可公開查詢

中　華　民　國 94 年 10 月 27 日

行政院國家科學委員會補助專題研究計畫 ■ 成 果 報 告 □期中進度報告

計畫名稱： 鑭錳氧化物/(絕緣氧化物,導體)異質微粒複合物中晶界自旋極化穿隧效應與磁傳輸機制的探討

計畫類別：■個別型計畫　　□ 整合型計畫
計畫編號：NSC 93－2112－M－164－003
執行期間：93 年 08 月 01 日至 94 年 07 月 31 日

計畫主持人：楊尚霖副教授兼系主任
共同主持人：
計畫參與人員：謝承達，張國興

成果報告類型(依經費核定清單規定繳交)：■精簡報告　□完整報告

本成果報告包括以下應繳交之附件：
□赴國外出差或研習心得報告一份
□赴大陸地區出差或研習心得報告一份
■出席國際學術會議心得報告及發表之論文各一份
□國際合作研究計畫國外研究報告書一份

處理方式：除產學合作研究計畫、提升產業技術及人才培育研究計畫、列管計畫及下列情形者外，得立即公開查詢
□ 涉及專利或其他智慧財產權，■一年□二年後可公開查詢

執行單位：修平技術學院

中　華　民　國　94　年　10　月　26　日

行政院國家科學委員會專題研究計畫成果報告

鑭錳氧化物/(絕緣氧化物,導體)異質微粒複合物中晶界自旋極化穿隧效應與磁傳輸機制的探討

Study of intergrain spin-polarized tunneling and extrinsic magnetotransport mechanism in manganite/(oxide, metal) heterogeneous granular composites

計畫編號：NSC 93-2112-M-164-003-
執行期限：93 年 8 月 1 日至 94 年 7 月 31 日
主持人：楊尚霖副教授兼系主任　　修平技術學院電機工程系
計畫參與人員：謝承達，張國興

1. Abstract

本研究係針對 $La_{0.7-x}Ln_xPb_{0.3}MnO_3$ (Ln=Pr, Nd, Dy, and Y)磁阻氧化物的磁傳輸特性的差異進行比較。研究結果顯示 La 由 Pr, Nd, Dy,和 Y 取代會造成磁電特性相當的影響。此趨勢和 Pr, Nd, Dy,和 Y 的離子半徑小於 La，且有不同的電子組態吻合。其中 Pr, Nd 系列化合物的飽和磁矩隨取代量增加而增加，而 Y 系列化合物的飽和磁矩隨取代量減少而減少，唯 Dy 系列先增加後減少。其原因在於 Pr, Nd 具有 f 層軌欲域電子對磁矩會有貢獻，故隨參雜量增加而增加，Y 不具有 *f* 層軌欲域電子對磁矩不會有貢獻，因此隨參雜量造成晶格扭曲而使磁矩下降。至於 Dy 系列，則是由兩種因素競爭比較而造成先增加後減少。**本研究結果已發表於 IEEE Transaction on Magnetics, Vol. 41, No. 10, 2005, pp. 2754。**對於晶界及其複合物的瓷磁電特已陸續完成投稿審查中。

關鍵字：鈣鈦礦，磁阻，電阻係數，晶界。

We present an investigation on the magnetic and transport properties of perovskite oxides, $La_{0.7-x}Ln_xPb_{0.3}MnO_3$ (Ln=Pr, Nd, Dy, and Y) in this study. The replacement of La by Pr, Nd, Dy, or Y results in a variation of magnetization process and magnetoresistance. The fact is in agreement with the smaller ionic radii of Pr, Nd, Dy, and Y ions in contrast to La ion and the difference of electronic configuration and effective moment. The saturation magnetization M_S increases as Pr or Nd content increases while M_S decreases as Y content increases. Moreover, the saturation magnetization M_S increases and then decreases as Dy content increases. These results can be explained in terms of the competition between the increase of ferromagnetically interacting spins due to the introduction of magnetic Pr, Nd, or Dy ions with *f*-shell electrons and suppression of ferromagnetism due to structure tuning induced by the small ionic radius of the interpolated cation into the La-site. The enhancement of magnetoresisance ratio as well as the increase of resistivity is observed for all systems. Result of double peaks temperature dependence resistivity for Dy and Y content systems is different from the result of the rest systems. The variation of electrical property is unduced by the grain boundary effect.

Keywords：perovskite, magnetoresisance, resistivity, grain boundary.

2. Introduction

Manganese oxides, $A_{1-x}A'_xMnO_3$ (A = La, Pr, Nd, Y etc., and A' = Ca, Sr, Ba, Pb etc.), with perovskite structure have attracted considerable investigation because of colossal magnetoresistance effects and industrial applications [1]-[4]. The partial substitution of divalent ions for the trivalent rare earth ions induces a paramagnetic to ferromagnetic phase transition explained by the double-exchange (DE) mechanism [5] in these compounds. Near the ferromagnetic transition temperature T_C, these oxides show a metal-insulator transition with a peak in the resistivity. There appears to be a direct relationship between the complex lattice effects and the transport properties in these perovskite compounds [6]. To evaluate the effect of rare-earth element substitution, we have made a systematic study on the magnetic and transport properties induced by La-site substitution. Dramatic variation of magnetic and transport properties induced by the La-site substitution is observed for these perovskites in this study.

3. Experimental

Polycrystalline oxide samples of the compounds, $La_{0.7-x}Ln_xPb_{0.3}MnO_3$ (Ln=Pr, Nd, Dy, and Y), were prepared by the conventional ceramic fabrication technique of solid-state reaction. The structure and phase purity of the samples were examined by the diffraction patterns recorded in the 2θ ranges from 20^o to 60^o with a powder diffractometer (Rigaku, PC-2000, Cu-Kα radiation) at room temperature. The magnetization measurements between 5K and 350K were performed in a quantum designed superconducting quantum interference device MPMS-5S SQUID magnetometer. The magnetization curves as a function of temperature in an applied field, μ_0H, of 5T were recorded. Resistivity was obtained from the standard four-point probe method on bars of typical dimensions 10mm×1.5mm×1mm. The applied field was parallel to the direction of electrical current. The resistivity curves as a function of temperature were collected with and without an applied field of 1T.

4. Results and Discussion

We have examined the magnetization process and magnetoresistance of manganite oxides, $La_{0.7-x}Ln_xPb_{0.3}MnO_3$ (Ln=Pr, Nd, Dy, and Y). It is interest for us to survay the size mismatch effect on the magnetic behaviors and transport properties when the Ln-site ions are smaller than La to fill the space in the octahedral MnO_6 and, consequently, results in a more distorted structure and Mn-O-Mn bond bending [7]. The parameters of La^{3+}, Pr^{3+}, Nd^{3+}, Dy^{3+}, and Y^{3+} with electronic configuration [Xe], $[Xe](4f)^2$, $[Xe](4f)^3$, $[Xe](4f)^9$, and [Kr], respectively, are listed in Table 1 [8].

Fig. 1 shows the magnetization curves as a function of temperature measured in an applied field of 5T for the $La_{0.7-x}Pr_xPb_{0.3}MnO_3$ and $La_{0.7-x}Nd_xPb_{0.3}MnO_3$ oxide systems. The samples undergo a paramagnetic to ferromagnetic transition as the temperature decreases. For both of the two systems, the saturation magnetization (M_S, defined as the magnetization at 5K and an applied field of 5T for comparison) increases with the increase of Nd or Pr content. In the Pr-doped compounds, the manganese sublattice is ferromagnetic and the magnetic ions, Pr^{3+}, with *f*-shell electrons are gradually aligned with

manganese as the temperature decreases. The magnetic Pr^{3+} ions contribute to an additional magnetization value (effective moment as listed in Table 1) to the total moment for Pr-doped samples. However, the spins of Pr^{3+} with *f*-shell electrons are hard to be fully aligned with those of Mn due to the deformation induced by the substitution of Pr for La (radii as listed in Table 1). As Fig. 1(a) shows, complete magnetic saturations for Pr-doped samples are not achieved even at 5K, which shows high dM/dT slope. For the Nd-doped compounds, similar behavior was also observed. However, due to the less unpaired *f*-shell electrons of Pr^{3+} than Nd^{3+}, the M_S values are smaller of Pr-doped compounds than those of Nd-doped ones as shown in Fig. 1(a) and (b).

The magnetization curves as a function of temperature for the $La_{0.7-x}Dy_xPb_{0.3}MnO_3$ system are shown in Fig. 1(c). For the Dy-doped system, the M_S increases initially with the increase of Dy content, reaches a maximum value for x = 0.1 and then decreases with the increase of Dy content. The results can be explained in terms of the competition between the increase of ferromagnetically interacting spins and suppression of ferromagnetism. As listed in Table 1, the effective moment value of Dy^{3+} is quite larger than that of La^{3+}, Pr^{3+} and Nd^{3+} and in a consequence the Dy^{3+} contributes to a more additional magnetization value to the total moment than Pr^{3+} and Nd^{3+}. This is the reason why M_S increases with the increase of Dy content due to the increase of ferromagnetically interacting spins initially. However, the radius of Dy^{3+} is quite smaller than La^{3+}, Pr^{3+} and Nd^{3+}. The introduction of Dy into La site induces heavy distortion of crystal structure and suppression of ferromagnetism. Complete magnetic saturations for Dy-doped samples are also not achieved even at 5K. The higher *d*M/*d*T slope values for heavy doped samples show that the suppression of ferromagnetism induced by structure distortion plays a primary role. Thus, the M_S decreases with the increase of doped content for $x \geqq 0.1$.

In contrast, M_S decreases with the increase of Y content in the Y-doped oxides as shown in Fig. 1(d). It can be inferred that the substitution of smallest Y^{3+} for La^{3+} can distort the perovskite structure and give rise to a larger bending angle of the Mn-O-Mn, which consequently weakens the ferromagnetic double exchange interaction between Mn^{3+} and Mn^{4+}. The effective magnetic moment is 0 μ_B for Y^{3+}, which is much smaller than those of Pr^{3+}, Nd^{3+}, Dy^{3+}. Therefore, the increase of ferromagnetism suppression induced by structure distortion with the increase of Y content plays a major role for Y-doped compounds and which is quite different from that of the rest compounds.

Fig. 2 shows the resistivity curves as a function of temperature obtained under the applied fields of 0T and 1T for Pr-doped and Nd-doped systems. The MR ratios at T_P are 17.2% at 332K (x=0.0), 18.5% at 321K (x=0.1), 28.9% at 289K (x=0.3), 35.2% at 149K (x=0.5), and 41.1% at 117K (x=0.7) for Pr-doped compounds and are 17.2% at 332K (x=0.0), 19.2% at 296K (x=0.1), 30.8% at 261K (x=0.3), 47.6% at 128K (x=0.5), and 66.7% at 95K (x=0.7) for Nd-doped compounds. It is found that the presence of Pr or Nd results in an increase of resistivity ρ and a lowering of the metal-insulator transition temperature T_P. The increase of resistivity can be explained by the deformation of structure induced by the smaller Pr or Nd

substitution for La and the corresponding deformation of crystal structure. Thus, the electron hopping across the Mn-O-Mn meets high resistance at zero-field. With an external field applied of 1T, resistivity decreases due to the suppression of spin scattering and enhanced magnetoresistance (MR) ratio, defined as $[\rho(0T)-\rho(1T)]/\rho(1T)$, is obtained. Thus, the MR ratio of doped compounds is larger than that of pure $La_{0.7}Pb_{0.3}MnO_3$. The reason holds for the increase of MR ratio and resistivity of Nd-doped system and larger values than those of Pr-doped system with the same doped content x. We observed an enhancement of MR with the increase of Pr or Nd content for both systems.

Fig. 3 shows the resistivity curves as a function of temperature for Dy-doped and Y-doped systems. The MR ratios at T_P are 17.2% at 332K (x=0.00), 18.9% at 316K (x=0.05), 19.8% at 201K (x=0.10), 22.4% at 182K (x=0.15), and 24.2% at 169K (x=0.20) for Dy-doped compounds and are 17.2% at 332K (x=0.00), 19.6% at 297K (x=0.05), 21.4% at 190K (x=0.10), 23.6% at 179K (x=0.15), and 25.2% at 152K (x=0.20) for Y-doped compounds. Larger increase of MR and resistivity than those of Pr-doped and Nd-doped systems is obtained with the same x. This result is obviously attributed to the smaller ionic radius of Dy and Y than the ionic radius of Pr and Nd. Result of double peaks temperature dependence resistivity curves for Dy and Y content systems is different from the result of the rest systems as shown in Fig. 2. The dissimilarity of electrical property shows a clear extrinsic magnetoresistance behavior. The competition between DE mechanism in the core of the grains (high temperature peak) and the tunneling magnetoresistance in the grain boundaries (low temperature peak) can explain the observed double peaks temperature dependence resistivity. Thus, the gradual obviousness of low temperature peak indicates that the transport mechanism is governed by the tunneling magnetoresistance rather than DE with the increase of Dy or Y content.

5. References

1. N. Shannon and A. V. Chubukov, Phys. Rev. B, vol. 65, pp. 104418, 2002.
2. S. L. Young, Y. C. Chen, H. Z. Chen, L. Horng and J. F. Hsueh, J. Appl. Phys., vol. 91, pp. 8915, 2002.
3. G. T. Tan, S. Dai, P. Duan, Y. L. Zhou, H. B. Lu, and Z. H. Chen, Phys. Rev. B, vol. 68, pp. 014426, 2003.
4. S. Zhang, L. Luan, S. Tan and Y. Zhang, Appl. Phys. Lett., vol. 84, pp. 3100, 2004.
5. C. Zener, Phys. Rev., vol. 82, pp. 403, 1951.
6. J. M. De Teresa, M. R. Ibarra, J. Garcia, J. Blasco, C. Ritter, P. A. Algarabel, C. Marquina, and A. D. Moral, Phys Rev. Lett., vol. 76, pp. 3392, 1996.
7. H. Y. Hwang, S-W. Cheong, P. G. Radaelli, M. Marezio and B. Batlogg, Phys. Rev. Lett., vol. 75, pp. 914, 1995.
8. R. D. Shannon, Acta. Cryst. A, vol. 32, pp. 751, 1976.

Table 1 Values of radius, effective moment and magnetism for trivalent lanthanide and yttrium ions.

Ion	Radius (nm)	Effective moment (μ_B)	Magnetism
La^{3+}	0.136	0	nonmagnetic
Pr^{3+}	0.130	3.58	magnetic
Nd^{3+}	0.127	3.62	magnetic
Dy^{3+}	0.120	10.63	magnetic
Y^{3+}	0.119	0	nonmagnetic

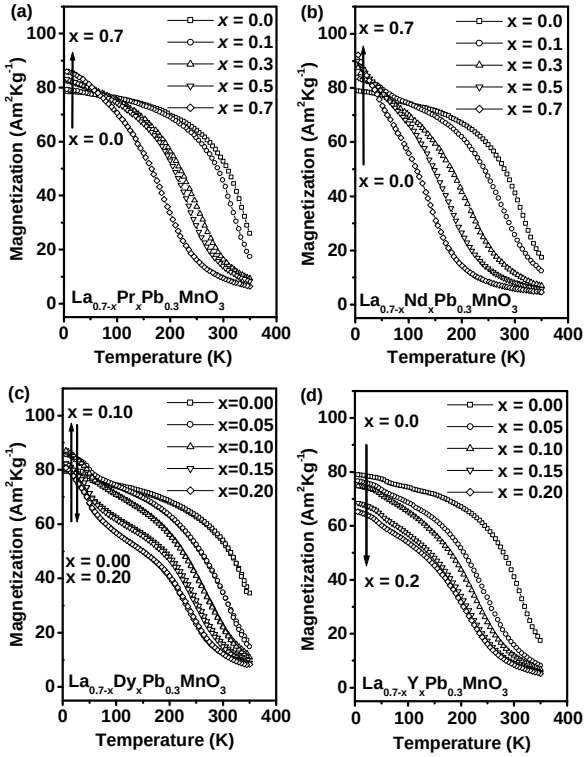

Fig. 1. Magnetization as a function of temperature for (a)$La_{0.7-x}Pr_xPb_{0.3}MnO_3$ (b) $La_{0.7-x}Nd_xPb_{0.3}MnO_3$ (c) $La_{0.7-x}Dy_xPb_{0.3}MnO_3$ and (d) $La_{0.7-x}Y_xPb_{0.3}MnO_3$ systems.

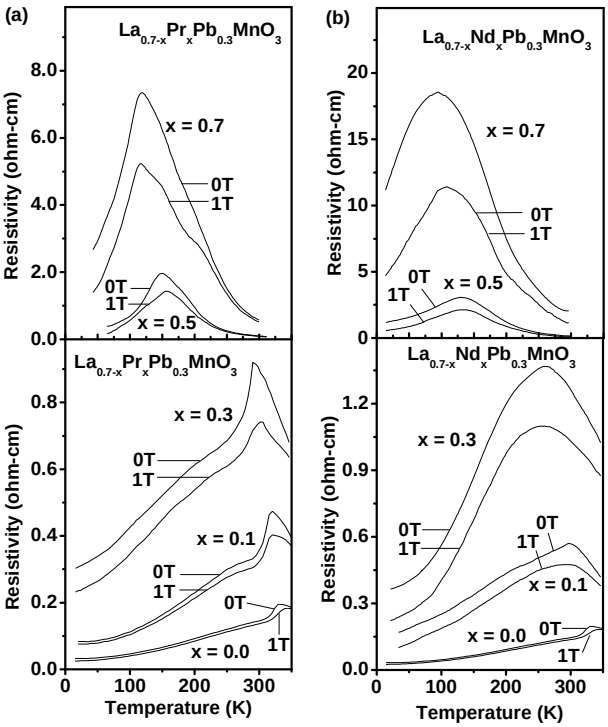

Fig. 2. Resistivity as a function of temperature for (a)$La_{0.7-x}Pr_xPb_{0.3}MnO_3$ (b) $La_{0.7-x}Nd_xPb_{0.3}MnO_3$ systems.

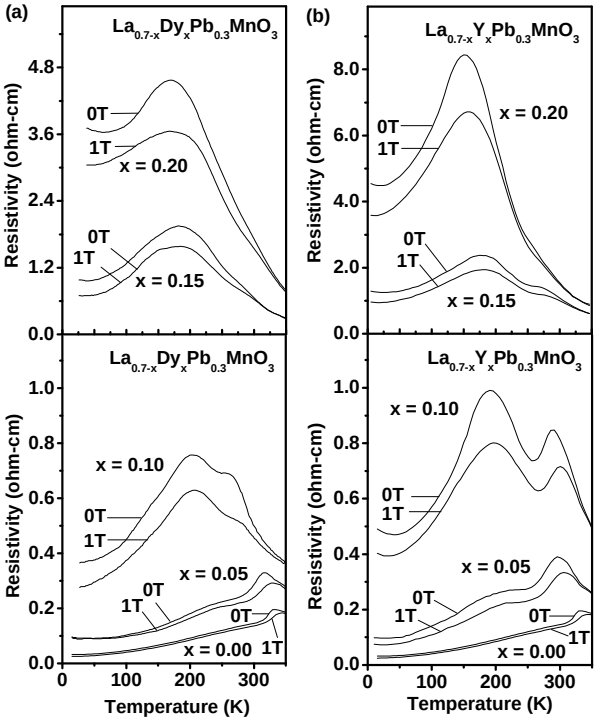

Fig. 3. Resistivity as a function of temperature for (a)$La_{0.7-x}Dy_xPb_{0.3}MnO_3$ (b) $La_{0.7-x}Y_xPb_{0.3}MnO_3$ systems.